Discontinuum Modelling of Blasting Process in Blocky Rock Media

Ali Mortazavi

ABSTRACT

The objective of this paper is to investigate, in a simplified manner, the process of rock blasting in discontinuous and blocky rock media. The developed code considers the effects of blast geometry (blasthole shape, angle, and location), the physical properties of the intact rock and existing discontinuities, and the blasthole pressure on the processes of rock breakage, fragment throw and muckpile formation. The newly modified DDA code (DDA_BLAST) describes the expansion of the blast chamber as a function of blast chamber volume and time. It is assumed in the code that the media consists of a blocky rock mass which is already fragmented in-situ due to the intersection of pre-existing discontinuities and the passage of stress wave. Hence, the model only considers the gas pressurization phase of the blasting process. Moreover, the proposed model for blasthole expansion assumes an adiabatic expansion of explosion products and variations in explosion pressure upon expansion of blast chamber is calculated from an equation of state. The newly developed DDA_BLAST code was employed to simulate a typical bench blasting problem in jointed rock mass and delve into the mechanisms involved (in a macro scale) in the gas pressurization phase of the blasting process.

KEYWORDS

Discontinuum modelling, Rock blasting, Rock mechanics, DDA, Bench blasting

1. INTRODUCTION

The process of rock breakage by blasting is a complex phenomenon, which is controlled by many variables and parameters. Considering all these parameters in a single analysis is not possible at the present time especially when some of them are not clearly understood yet and the effect of others is difficult to quantify. With regard to the complexity of geomaterials, various attempts have been made to conceptualize the mechanisms of rock fragmentation by blasting. These studies were conducted in the forms of empirical or semi-empirical techniques and were used for blast design and prediction of rock fragmentation. In most of these studies, the behaviour of the materials used (e.g. Plexiglas, concrete, etc.) was much better characterized and known than that of the actual material of concern (rock). Therefore, with regard to the above discussion and ease of access to powerful computers, it would be beneficial to develop numerical models to further understand and predict the rock fragmentation process. The objective of this paper is to introduce the development of a dynamic blasthole expansion code, which is coupled to the discontinuous deformation analysis (DDA) code of Shi (1988). The application of the new code to a typical blasting problem is also demonstrated.

2. DISCONTINUOUS DEFORMATION ANALYSIS

Discontinuous Deformation Analysis (DDA) is a method that has been introduced by Shi (1988) to analyze the mechanical behavior of blocky systems. The interactions between blocks in DDA are simulated by springs or penalties and a system of simultaneous equations is formulated by minimizing the total potential energy of the system. DDA is an implicit method in which displacements are the unknowns to be solved. The original DDA code uses a first order displacement function to describe the block deformation. Total block deformation consists of six components; two rigid body translations in the x and y directions, one rotational component, normal strain in the x and y directions, and the shear strain component. All these deformational components are represented in the matrix formula form shown below:

A. Mortazavi is with the Department of Mining Engineering, Amirkabir University of Technology, Tehran, Iran (e-mail: mortazav@aut.ac.ir).

$$\begin{pmatrix} u \\ v \end{pmatrix} = \begin{pmatrix} 1 & 0 & -(y-y_o) & x-x_o & 0 & (y-y_o)/2 \\ 0 & 1 & x-x_o & 0 & y-y_o & (x-x_o)/2 \end{pmatrix} \begin{pmatrix} u_o \\ v_o \\ r_o \\ \varepsilon_x \\ \varepsilon_y \\ \gamma_{xy} \end{pmatrix} = [T][D] \quad (1)$$

where u & v = displacement in the x and y directions; $[T]$ = displacement function; $[D]$ = matrix which contains 6 displacement variables. Individual blocks in DDA can form a blocky system through simulated contacts (use of springs) between them. Shi (1988) showed that for n blocks in the system, the simultaneous equilibrium equations can be written in matrix form as follows:

$$\begin{bmatrix} K_{11} & K_{12} & K_{13} & \cdots & K_{1n} \\ K_{21} & K_{22} & K_{31} & \cdots & K_{2n} \\ K_{31} & K_{32} & K_{33} & \cdots & K_{3n} \\ \vdots & \vdots & \vdots & \ddots & \\ K_{n1} & K_{n2} & K_{n3} & \cdots & K_{nn} \end{bmatrix} \cdot \begin{bmatrix} D_1 \\ D_2 \\ D_3 \\ \vdots \\ D_n \end{bmatrix} = \begin{bmatrix} F_1 \\ F_2 \\ F_3 \\ \vdots \\ F_n \end{bmatrix} \quad (2)$$

where K_{ii} = stiffness coefficient of block i; K_{ij} = coefficient of contacts between blocks i and j. The system of Equation (2) is solved for the displacement unknowns and the solution is controlled by contact constraints associated with block kinematics (i.e. no tension and penetration are allowed between blocks). Coulomb's law is used to interpret sliding along interfaces and represents energy loss due to friction.

3. BLAST MODELLING

A. Blast loading mechanism

The detonation process creates a reaction front traveling at a speed, which exceeds the velocity of sound in the material. This process generates temperatures in the order of 1600° C -3800° C and pressures between 1000-27000 MPa just behind the detonation front. The detonation process can be considered as a self-sustaining reactive shock wave, which results in a shock pressure, transmitted into the adjacent rock at characteristic velocities of 3000-6000 m/s (Mohanty & Chung, 1986). This process creates a pressure front that propagates a stress wave into the surrounding rock at a very high speed. Depending on the strength, physical properties, and degree of inhomogeneity of rock, the stress wave action varies significantly. In damaged, fractured rock masses, the stress wave gets attenuated very rapidly and fragmentation due to the wave action is very limited. In contrast, in competent hard rocks, upon propagation of compressive stress wave and its reflection from free boundaries, stresses occur in rock in the normal and tangential directions that exceed the rock's tensile strength and cause radial fracturing.

After the stress wave generation and propagation stage is over, extremely high-pressure gases, generated during the detonation process, start to impact the blasthole walls and force a path through pre-existing discontinuities and the stress-wave-induced radial cracks. This process increases the stress level at the surrounding rock and further propagates the created fractures. The fracturing of the material continues up to the free face and at the same time burden detachment and movement occurs. Subsequently, gases vent to the atmosphere and the last portion of explosive energy is lost in the forms of heat and noise.

Therefore, with regard to the above discussion, the process of rock breakage by blasting can be broadly categorized into two major stages of stress wave loading phase and gas pressurization phase. It is understood that in practice there is a relatively unknown and complex transition stage between these two phases, but this is ignored for the sake of simplicity. Furthermore with regard to the nature of blocky rock media, the role of stress wave is ignored in the analysis and only the second phase of the blasting process (i.e. gas pressurization phase) was investigated. In other words, this work presumes that the rock is already fragmented in-situ due to the intersection of pre-existing discontinuities and the action of stress waves. Hence, the main concern of the paper is to study only the gas pressurization phase of the blasting process, which according to many researchers (Persson et al., 1969; Hagen, 1983; Brinkman, 1978; Haghighi et al., 1988; Kutter & Kulozik, 1990; Mortazavi & Katsabanis, 2001) involves most of the blast energy in jointed media.

B. Energy partitioning in blasting

It is believed that in discontinuous and blocky media it is the gas pressurization action that causes most of rock breakage. At this stage the entire explosive column has burned into high-pressure gases and the blasthole has expanded slightly due to the action of the stress wave. Energy partitioning diagram of Lownds (1986) and Udy & Lownds (1990) can be used to describe the blasting process. With the aid of this model, which is based on the assumptions that rock behaves elastically and the explosion in rock is an adiabatic phenomenon, interactions of various explosives with various rock types can be analyzed. This diagram is illustrated in Figure 1.

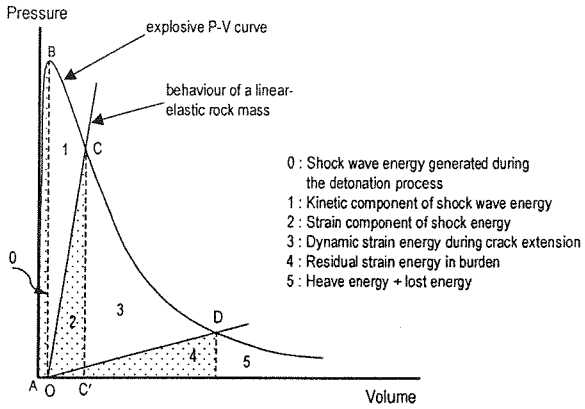

Figure 1: Simplified energy partitioning during blasting in a continuous rock mass (Udy and Lownds, 1990)

The detonation process starts at point *A* (time zero) and the detonation front propagates through the explosive column. At point *B* the explosive column is fully burnt into high-pressure gases and the generated shock wave has impacted the blasthole walls. During the generation and propagation of the shock wave until the peak blasthole pressure is reached (point *B*) the blasthole expands slightly. The impact of the detonation products with the blasthole wall creates a compressive stress field in the surrounding rock leading to propagation of a stress wave into the medium. During propagation and reflection of the stress wave from boundaries, part of its energy is consumed in crushing and fracturing around the blast-hole and spalling at the free faces. This component of energy can be represented by area 1 of Figure 1. The remaining part of the stress wave energy, which is stored as strain energy in the rock, can be illustrated by area 2. During the stress wave loading stage, the rock properties change locally resulting in further expansion of the blasthole (up to point *C*). At point *C*, in which the rock is at equilibrium state (Udy & Lownds, 1990) with the stresses induced by the stress wave action, the effective radius of the blasthole for the action of high-pressure gases is defined. At this stage (Point *C*), the material beyond the crushed zone is still intact and stationary, but under high internal stresses. After point C the energy of the high-pressure detonation products is fully mobilized and the rock cannot resist the full fracturing of the burden anymore. According to Udy & Lownds (1990), the burden begins to detach only after cracks originating at the blasthole reach the free face or after the gas entering and opening new and pre-existing cracks reaches the free face or both. The expansion process and fragmentation from point *C* to *D* are associated with the gas pressurization phase as well as the release of the strain energy stored in the rock by stress wave and gas. At point *D*, which represents the pressure of the gases at escape, the load-bearing capacity of the rock mass is significantly deteriorated due to the fragmentation process. This can be understood schematically from the slope of line *OD*, however, individual rock fragments have gained significant kinetic energy at this point. After point *D* the remaining part of the blast energy is consumed in the forms of heave, noise, venting through free faces, and fly rock.

C. Blasthole expansion model

Modelling of the interactive behaviour of the detonation products and the surrounding medium is a major requirement for rock blasting analysis. It is assumed here that the explosion gases behave ideally and no heat losses occur. The pressure of the detonation products depends on the expansion of the blast chamber and open cracks, which in turn is related to the properties of the surrounding material. Therefore, the interactive modelling of volume (expansion of gases) and pressure of the gases is essential in the simulation of the process. The instantaneous pressure of the explosion gases at any time during the expansion process is calculated using a simple power law equation of sate (EoS). It is recognized that better EoS exist to describe the *P-V* relationship of the detonation process. However, the power law equation of state is used in the current analyses for simplicity and has the following form:

$$P = P_{\circ}\left(\frac{V_{\circ}}{V}\right)^{\gamma} \qquad (3)$$

where P_o and V_o are the initial pressure and volume of the explosion gases respectively. P and V represent the final state of the expansion and γ is a constant to be determined either experimentally or through hydrodynamic calculations. From experimental results the constant, γ, is expected to be in the range 1.2-3.0 for high temperature and high densities of gas that occur in practice (Paine & Please, 1994). This adiabat can be predicted using ideal thermo-hydrodynamic codes or by performing cylinder expansion tests when ideal explosives are used. For non-ideal explosives, alternative techniques must be used to generate a complete equation of state of the detonation products.

The expansion model presented here is based on dynamic tracking of rock blocks, which are located around the blasthole. A simplified concept of the model is illustrated by Mortazavi et al. (2001). In this model, after the explosion had occurred, the gas pressure is uniformly applied to the block edges, which form the blasthole chamber. Then, these pressurized blocks push the surrounding blocks outward and energy is exchanged between all blocks. Accordingly, the blast chamber expands and obtains a new geometry with gas pressure acting on it. As the chamber expands, blocks located around the chamber may undergo translation in the x and y directions, rotation about their mass center, and normal and shear straining. The excessive straining and deformation of blocks surrounding the chamber are treated in the model, however, the fracturing process is not

considered in the current version of the model.

The model precisely tracks deformation and displacement of the blocks that surround the blast chamber. Once the gas loads an open discontinuity, the discontinuity is going to be further opened and propagated. Consequently, adjacent discontinuities will be squeezed and closed. Depending on the number of blocks that surround the blasthole, any number of discontinuities in any direction (outward from the chamber) and up to any length (constrained by the whole geometry of the model) can be opened and propagated by the gases. However, because of the plane strain loading assumption and the two-dimensional approach of the model, the gas penetration distance is limited to a certain distance from the blasthole. With regard to the blast geometry (blasthole length, burden, stemming) and the size of the blocks, the gas penetration domain can be input to the model by the user.

D. Formulation of gas loading components

With regard to the first order displacement function used in the DDA method, the edges of blocks are always straight lines and no bending is allowed. As mentioned earlier, knowing the block edges, which are pressurized, the gas pressure is applied on blocks in the appropriate direction. It is obvious that the blast chamber does not expand uniformly in all directions. Depending on material properties and strength parameters of joints (friction angle, cohesion, tensile strength), the walls of the chamber dislodge differently. Assuming that the gas load is distributed on a straight block edge from point (x_1, y_1) to point (x_2, y_2), the parametric equation of the loading line can be written in the following from:

$$x=x_1+(x_2-x_1)\cdot t\,,\ y=y_1+(y_2-y_1)\cdot t \ \text{ and } \ 0\le t\le 1 \qquad (4)$$

where t is a positive real number representing the location on the line(0 and 1 values of t represent the two ends of the loading line). Then, the loading can be defined by:

$$F_x = F_x(t)\,, \qquad F_y = F_y(t)\,, \qquad 0 \le t \le 1 \qquad (5)$$

where functions $Fx(t)$ and $Fy(t)$ can be variant loading functions acting on the line (edge of a block). The potential energy of the line loading ($Fx(t)$, $Fy(t)$) is calculated as follows:

$$\Pi_i = -[D_i]^T \int_0^l [T_i]^T \begin{pmatrix} F_x(t) \\ F_y(t) \end{pmatrix} l\, dt \qquad (6)$$

where matrices $[D]$ and $[T]$, for block i, are defined in Equation (1) and l is the length of the loading line. The derivatives of the above energy function are computed with respect to the deformation variables to minimize the induced potential energy (equilibrium state). This, in turn, represents the equilibrium state of block i due to line loading. Since it is assumed that the gas force acts uniformly and as a constant force on block edges, Equation (6), after differentiation, reduces to the following formula for the gas loading components:

$$f_{gas} = \int_0^l [T_i]^T \begin{pmatrix} F_x \\ F_y \end{pmatrix} l\, dt \qquad (7)$$

Computing the integral of components of matrix $[Ti]$, the following 6 × 1 force sub-matrix can be determined for loading of block i:

$$(f_{gas})_{6\times1} = l \begin{pmatrix} F_x \\ F_y \\ -\frac{1}{2}(y_2+y_1-2y_o)F_x+\frac{1}{2}(x_2+x_1-2x_o)F_y \\ \frac{1}{2}(x_2+x_1-2x_o)F_x \\ \frac{1}{2}(y_2+y_1-2y_o)F_y \\ -\frac{1}{4}(y_2+y_1-2y_o)F_x+\frac{1}{4}(x_2+x_1-2x_o)F_y \end{pmatrix} \qquad (8)$$

The calculated six force components are associated with two translation components, one rotation component, and three straining components of deformation of block i. The matrix of Equation (8) is added to the global force matrix of Equation (2) and the global equation is solved for the unknown associated displacements. Accordingly, the interactions of loaded blocks with other blocks are evaluated by the DDA program calculating total deformation of all blocks. The above formulation is suitable in modelling of gas impact on the main blasthole chamber as well as the discontinuities, which are located in the close vicinity of the blast chamber. As the radial distance from the blasthole increases, the gas pressure drops in an exponential fashion by several complex mechanisms. These mechanisms are not clearly known at the present time; if the exact blasthole pressure-distance relationship could be obtained, it can be incorporated into the above formulation with no difficulty.

E. Modelling the effect of burden size on variations in blasthole pressure, blasthole volume, throw, and venting of the explosion gases

E1. Geometric description of the problem and input data

A typical bench blast geometry was considered for the analysis. The rock mass was intersected by two joint sets, which were oriented in the vertical and horizontal directions. The joint sets had a spacing of 0.5 m and a friction angle of 15°. Zero cohesion and tensile strengths were considered for the joints. The geometry of the model is shown in Figure 2. The power law equation of state (3) was employed in this model and a γ value of 1.8 was used for this example. The blasthole had a radius of 10 cm and a length of 5.8 m as shown in Figure 2. The stemming length was kept at 1.8 m and the burden distance was

varied from 1.5 m to 4 m. Since it was the intention of this example to study the effects of burden on the blasthole expansion and throw, a constant spacing of 2 m and an initial blasthole pressure of 1 GPa were considered for the whole analysis. The intact rock blocks were assumed to have a Young's modulus of 30 GPa, Poisson's ratio of 0.16, and density of 3.8 ton/m3.

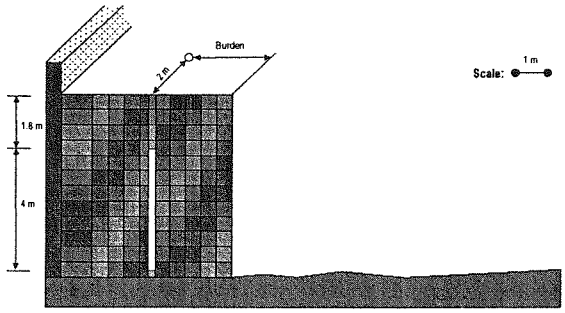

Figure 2: Geometry of model used in burden analysis

E2. Simulation results and discussion

The model was executed while maintaining a constant value for all input parameters with the exception of the burden size. DDA_BLAST simulation results for varying burden distances are presented in Figure 3 to Figure 6. Figure 3 to Figure 6 show the complete processes of blasthole expansion, burden detachment, movement, and throw for the simulated models. In order to have a better insight into the influence of the burden distance on the breakage process of the burden, the blasthole chamber volume and the blasthole chamber pressure were monitored versus time for the simulated bench blasts. The variation of the blast chamber volume versus time is presented in Figure 7 and Figure 8 illustrates the blast chamber pressure history for the simulated blasts.

When a small burden distance was employed, as shown in Figure 3, the force of the gases easily surmounted the inertial resistance of the burden. The blasthole expanded significantly and relatively quickly compared to the other cases. This can be seen from the rapid change in the gradient of the volume curve associated with 1.5 m burden distance (Figure 7). Moreover, this effect is also reflected in the blast chamber pressure versus time diagram of the model (Figure 8). Another interesting point about this model (B = 1.5 m) is the smoothness of the blast chamber volume/pressure-time diagrams. This shows that due to the speed of the process and little resistance of the burden, the dominant force of the gases uniformly and smoothly deformed the burden. The interactions of blocks were fully controlled by the gas force and since a small number of blocks were involved, the rock mass behaved less non-linearly compared to the other cases (larger burdens). The opening of the burden occurs at its mid-point due to significant bending (Figure 3, step 252-440), however, with regard to Figure 8, the pressure has already dropped to zero due to large expansion at the time of venting. Accordingly, the throw distance became large and a flat muckpile was formed.

As the burden distance was increased, the expansion rate decreased and the rock mass behaved slightly differently. The gases tried to force a path to the atmosphere through the stemming column rather than opening a path in the burden. At a larger burden distance of 2.5 m, the inertial resistance of the burden affected the blasthole expansion rate (Figure 4). Moreover, the non-linear behaviour of the discontinuous rock mass started to appear as shown in Figure 7. Lack of smoothness of the blasthole volume-time diagrams at larger burden distances is associated with irregular slips along the interfaces of the blocks that surround the blast chamber. Local and sudden increases in the blasthole volume shown by the volume-time diagrams are related to the abrupt outward displacements (away from the blasthole) of certain blocks along their interfaces. In contrast, local sudden drops in the blasthole volume, along the volume-time curves, are once again associated with the slippage of the individual blocks toward the blast chamber, thus reducing the chamber volume. The reason for this is the overall interaction and response of the block system against the applied gas load. The preceding discussion also holds for the blasthole pressure history since it is directly related to the blast chamber volume. The above effects are also reflected in the blasthole pressure-time diagrams of the simulated blasts, as shown in Figure 8. Furthermore, at larger burden distances (Figures 5 - 6), the gases sought a path to the atmosphere through the stemming area rather than through the burden and bench face.

The simulated models of larger burden distances (3-4 m), showed an obvious drop in the rate of blasthole expansion. Consequently, the gas pressure in the blasthole stayed high for a longer period, before venting occurred, in comparison to the smaller burden distances (Figure 8). For instance, at a burden distance of 3.5-4 m, due to the inertial resistance of the burden and the numerous block interactions (which dissipated a lot of energy), the blasthole expanded at a slower rate. As it is shown in Figure 8, at a certain time interval (6-9 ms) there is a relatively small drop in the blasthole pressure. It is the author's belief that this is associated with the block interactions and deformations within the burden rock mass while the whole burden is under a state of high stress but still stationary. Once the individual blocks in the burden have interacted and reached a local equilibrium state, the whole mass of the burden moves and results in further blasthole expansion. It should be realized that, at large burden distances, although the rate of blasthole expansion and pressure drop is lower, the gases vent much quicker through the stemming column. Also full bending of the burden is not happening due to lack of enough energy transmitted into the rock. This leads to an incomplete detachment of the burden and as a result toppling of the

burden without significant throw. This is a typical practical problem that generally occurs as a result of bad blast design.

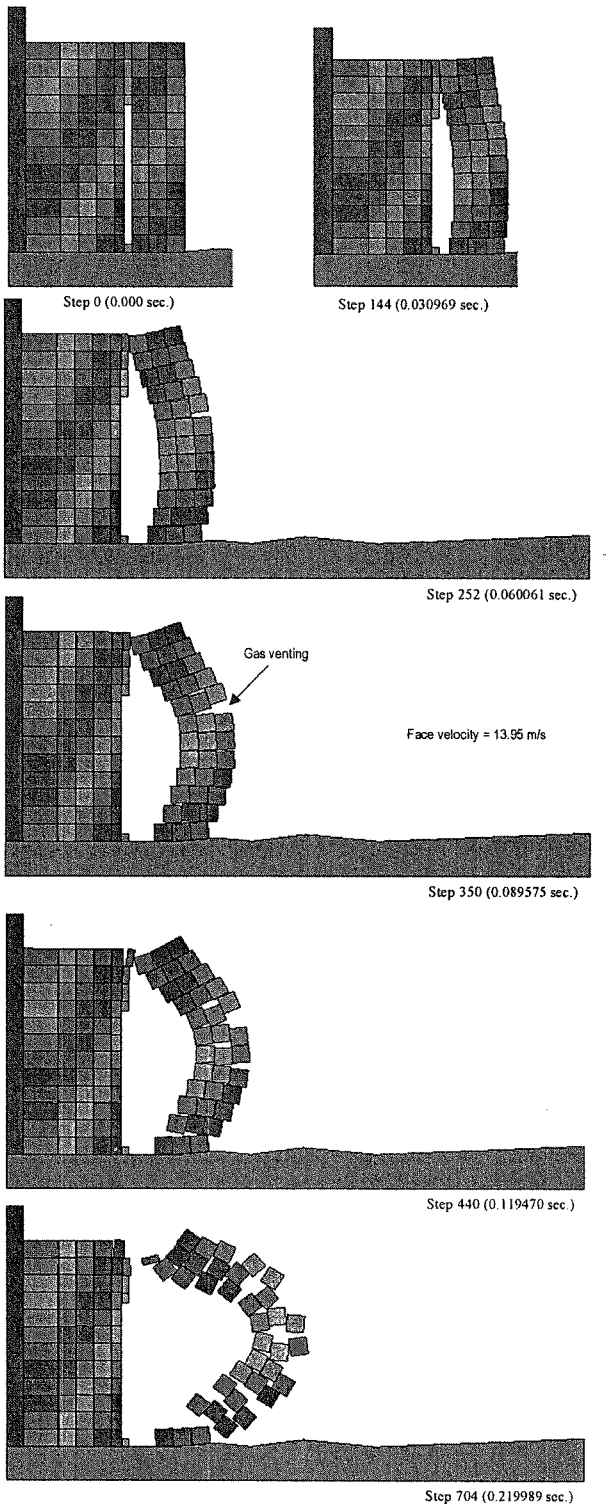

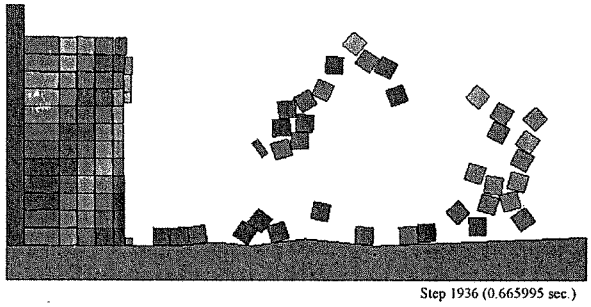

Figure 3: DDA_BLAST simulation results of a single blasthole bench (B = 1.5 m)

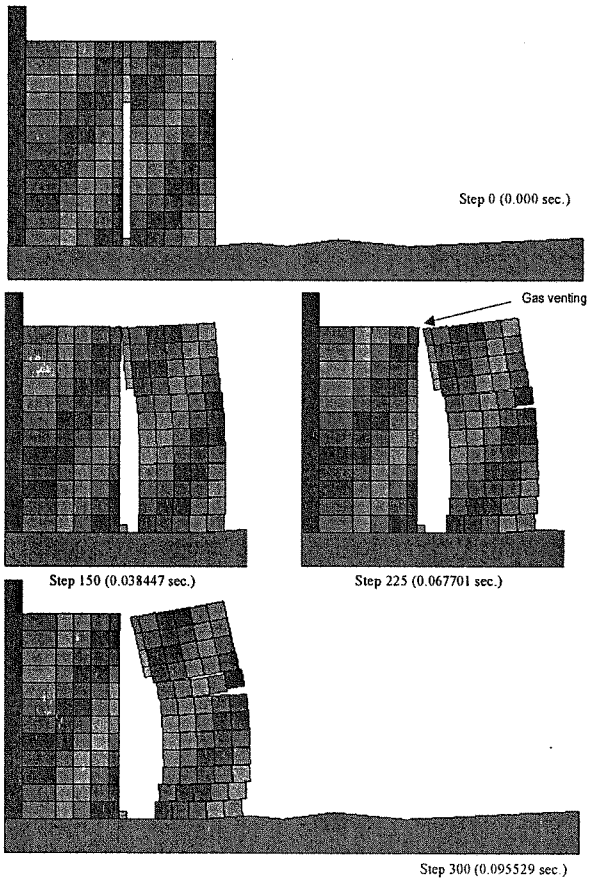

Figure 4: DDA_BLAST simulation results of a single blasthole bench (B = 2.5 m)

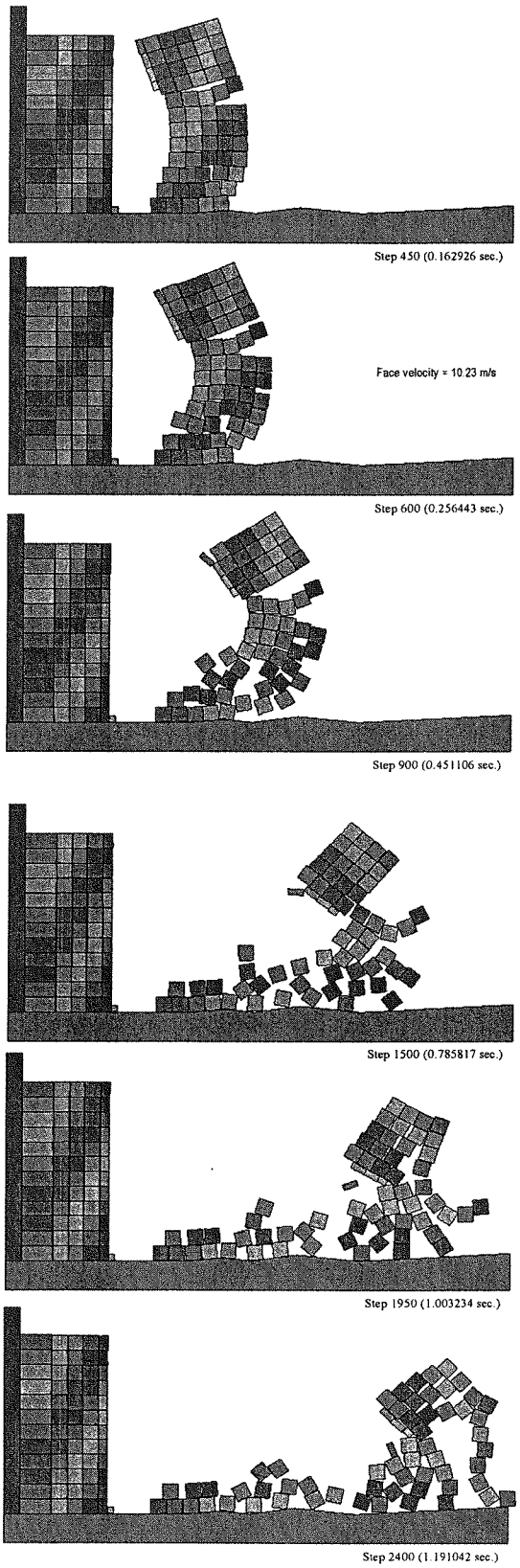

Figure 5: Continued from Figure 4

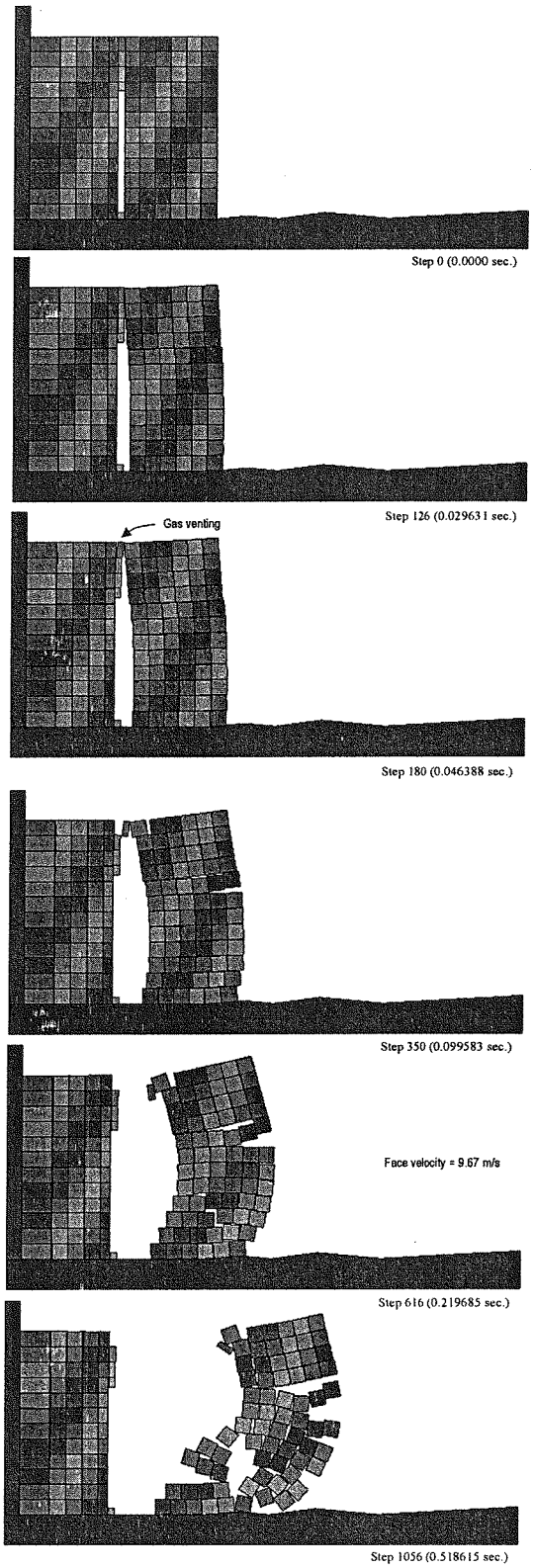

Figure 6: DDA_BLAST simulation results of a single blasthole bench (B = 3 m)

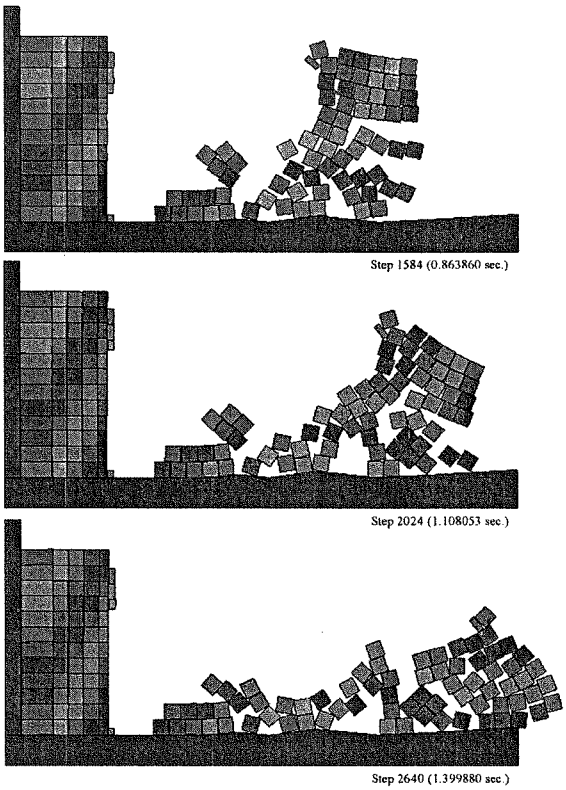

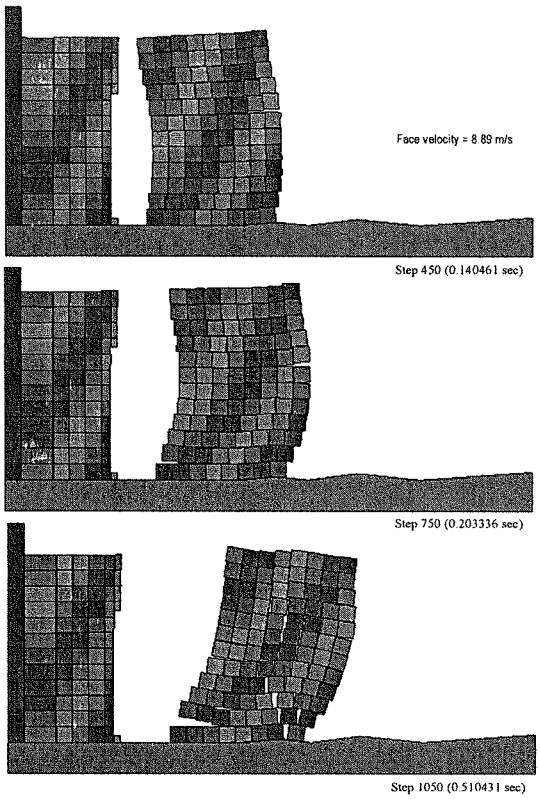

Figure 7: Continued from Figure 6

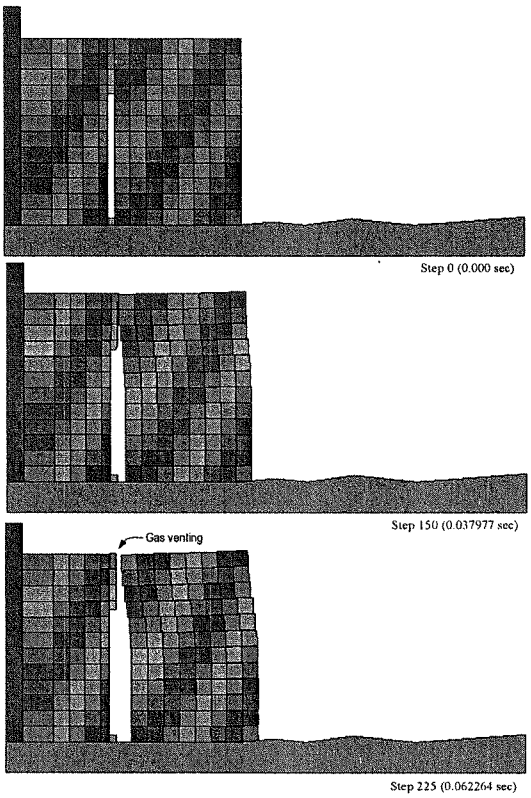

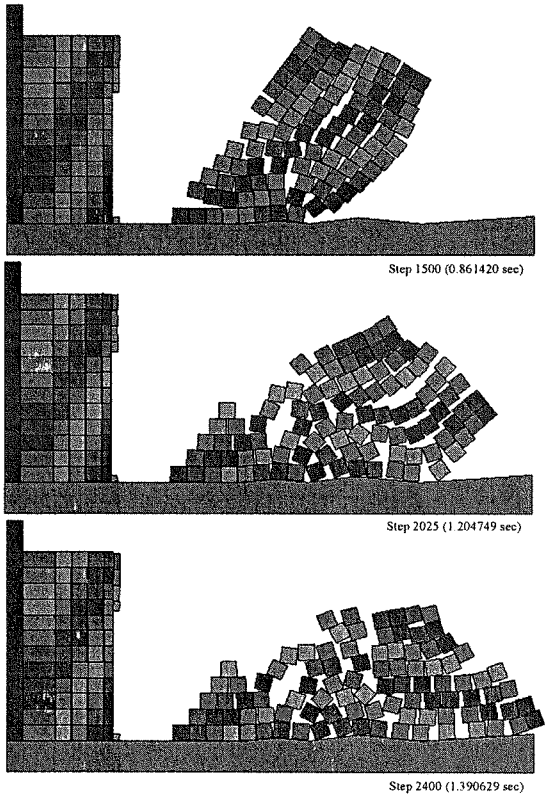

Figure 8: DDA_BLAST simulation results of a single blasthole bench (B = 4 m)

Another interesting point that can be speculated from Figures 7 and 8 is the initial expansion of the blasthole under applied gas load. It is evident that at times of 0 to 6 ms after detonation the blasthole expansion variations as well as the blasthole pressure changes are the same for all models. This initial expansion is due to the internal deformation of the blocks that surround the blasthole. Since material physical and mechanical properties and the initial input pressure are the same for all models, the same expansion and pressure history were observed for all of them. This fact signifies the importance of the block deformability in the immediate vicinity of the blasthole. If the blocks were modelled absolutely rigid, the initial stage of expansion process would have been modelled inappropriately. Alternatively, if the blocks were made fully deformable by either discretizing the individual blocks into finite element zones or implementing a higher order displacement function into the DDA formulation, the expansion of the blasthole could have been modelled more realistically. Figure 9 is a plot of face velocity versus burden distance for the simulated bench blasts. At small burdens (1.5-2 m), gases easily overcame the inertial resistance of the jointed rock mass. This led to relatively high face velocities. As the burden was increased, the inertial resistance of the burden increased and the rock mass, even though jointed, resisted the gas force and controlled the process by dissipating the energy through block interactions and deformations. This resulted in lower face velocities as shown in Figure 9.

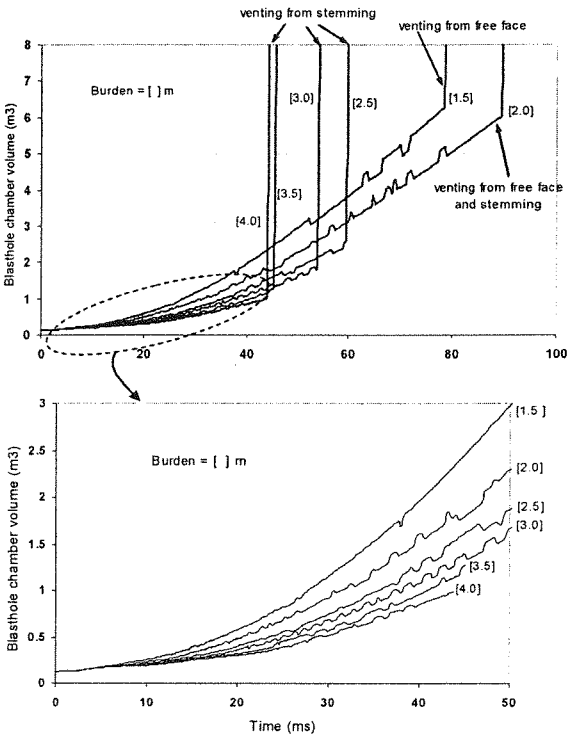

Figure 9: Variations of blast chamber volume versus time for varying burden distances

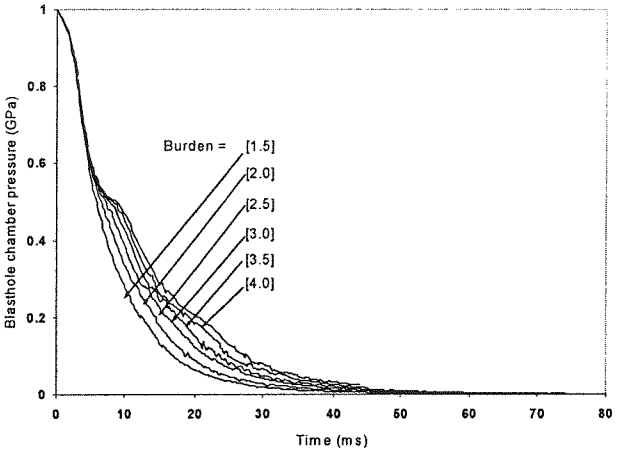

Figure 10: Variations of chamber pressure versus time for varying burden distances

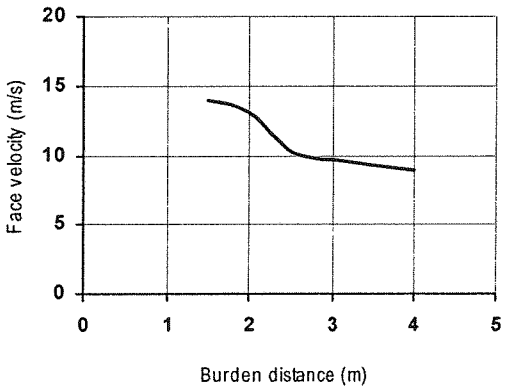

Figure 11: The effect of burden distance on face velocity

F. Discussion and Conclusions

In brief, the simulated examples clearly demonstrate the influence of the burden distance on the blasthole expansion, blasthole pressure history, mechanism of burden breakage, and throw. Using the DDA_BLAST code, for a given set of initial blasthole pressure, rock mass joint configuration, rock mass physical and mechanical properties, spacing distance, and stemming column, the optimum burden distance can be found by running the model for various scenarios and observing the results. The objective of the simulated example was to evaluate the effects of the burden distance on the pressure history experienced at the blasthole walls, the volume history of the blast chamber, the venting time of the explosion gases, and the throw of the burden material. The obtained results clearly showed the effects of the inertial resistance of the burden on the blasthole pressure, expansion of the blasthole, and venting of the explosion products. Additionally, the effects of the deformability of the intact blocks, surrounding the blasthole, as well as the deformability of the rock mass (assembly of all blocks) on

the pressure and volume history of the blast chamber were demonstrated. Moreover, non-linear behaviour of the jointed rock mass under applied gas load was demonstrated through the obtained blasthole volume versus time diagrams (Figure 7). The influence of the burden distance on the face velocity was also illustrated.

4. REFERENCES

[1] R. Haghighi, R.R. Briton, D. Skidmore, "Modelling gas pressure effects on explosive rock breakage," *Int. J. of Mining & Geological Engineering, Vol. 6, 73-79*, 1988.

[2] A Mortazavi, P. D. Katsabanis, "Modelling the influence of joint orientation and continuity on the process of rock breakage by blasting," *Int. Journal of Blasting and Fragmentation, Vol. 33 (4)*, 2001.

[3] B. Mohanty, S.H. Chung, "Developments in blasting physics-the current research focus," *Journal of Mines, Metals, and Fuels, 477-487, 1986.*

[4] A.S. Paine, C.R. Please, "An improved model of fracture propagation by gas during rock blasting: Some analytical results," *Int. J. Rock Mech. Sci. & Geomech. Abstr., Vol. 31, 699-706*, 1994.

[5] P.A. Persson, A. Ladegard-Pederson, B. Kihlstrom , "The influence of borehole diameter on rock blasting capacity of an extended explosive charge," *Int. J. Rock Mech. & Mining Sci. Geomech. Abstr., Vol. 6, 277-284*, 1969.

[6] J.R. Brinkman, "Separating shock and gas expansion breakage mechanisms," in *Proc. 1987 2nd Int. Symp. on Rock Fragmentation by Blasting, Keystone, Colorado*, pp 6-15

[7] T.N. Hagan, "The influence of controllable blast parameters on fragmentation and mining costs," in *Proc. 1983 the 1st Int. Symp. on Rock Fragmentation by Blasting, Lulea, Sweden*, pp 31-51.

[8] H.K. Kutter, R.G. Kulozik, "Mechanics of blasting in discontinuous rock mass," in *1990 Mechanics of Jointed & Faulted Rock (Edited by Rossmanith)*, pp 295-304.

[9] C.M. Lownds, "The strength of explosives," in *Proc. 1986 SAIMM The planning and operation of open pit and strip mines, J.P. Dectlefs (ed.), Johannesburg,* , pp 151-159.

[10] L.L. Udy, C.M. Lownds, "The partition of energy in blasting with non-ideal explosives," in *Proc. 1990 3rd Int. Symp. on Rock Fragmentation by Blasting, Brisbane, Australia*, pp 37-43.

[11] G.H. Shi, "Discontinuous Deformation Analysis," Ph.D. Thesis, Dept. Civil Eng., University of California at Berkeley, Berkeley, U.S.A, 1988.